Multi-Cluster based Dynamic Channel Assignment for Dense Femtocell Networks

Se-Jin Kim[1], IlKwon Cho[2], ByungBog Lee[3], Sang-Hyun Bae[1] and Choong-Ho Cho[4]
[1] Department of Computer Science and Statistics, Chosun University
Gwangju 501-759, Korea
[e-mail: sjkim@chcho.ac.kr]
[2] Department of Network Planning, National Information Society Agency (NIA),
Seoul 100-775, Korea.
[3] IoT Research Division, Electronics and Telecommunications Research Institute (ETRI),
Daejeon 305-700, Korea
[4] Department of Computer and Information Science, Korea University,
Seoul 136-713, Korea
[e-mail: chcho@korea.ac.kr]
*Corresponding author: Choong-Ho Cho

Received November 20, 2015; revised February 4, 2016; accepted February 5, 2016; published April 30, 2016

Abstract

This paper proposes a novel channel assignment scheme called multi-cluster based dynamic channel assignment (MC-DCA) to improve system performance for the downlink of dense femtocell networks (DFNs) based on orthogonal frequency division multiple access (OFDMA) and frequency division duplexing (FDD). In order to dynamically assign channels for femtocell access points (FAPs), the MC-DCA scheme uses a heuristic method that consists of two steps: one is a multiple cluster assignment step to group FAPs using graph coloring algorithm with some extensions, while the other is a dynamic subchannel assignment step to allocate subchannels for maximizing the system capacity. Through simulations, we first find optimum parameters of the multiple FAP clustering to maximize the system capacity and then evaluate system performance in terms of the mean FAP capacity, unsatisfied femtocell user equipment (FUE) probability, and mean FAP power consumption for data transmission based on a given FUE traffic load. As a result, the MC-DCA scheme outperforms other schemes in two different DFN environments for commercial and office buildings.

Keywords: OFDMA-FDD, Femtocell networks, Dynamic channel assignment, Multiple clustering, Graph coloring, Interference mitigation.

This research was supported by a research grant from the Institute for Information & Communication Technology Promotion(IITP) [No. R0101-15-0116].

http://dx.doi.org/10.3837/tiis.2016.04.004 **ISSN : 1976-7277**

1. Introduction

According to recent reports, mobile data traffic volume from smart phones, tablets, and so on is growing dramatically and more than 80% of them occur in indoor environments [1, 2]. In order to solve these problems, the femtocell network has become a promising solution since femtocells improve both the system capacity and coverage with low cost and low energy consumption [3-6]. Therefore, the world's major mobile network operators (MNOs) have been showing a great deal of attention to adopt femtocells for next generation mobile networks such as 3GPP LTE/LTE-Advanced [7-9] and IEEE 802.16m [10, 11]. However, in spite of the advantages of femtocells, various technical challenges still remain to enhance system performance. Channel assignment considering interference mitigation is one of the main issues because femtocell access points (FAPs) use the licensed spectrum owned by the macrocell network, and thus have cross-tier and co-tier interference from macro base stations (MBSs) and neighbor FAPs, respectively [12, 13].

In recent literature, several channel assignment schemes have been studied for femtocell networks. Early channel assignment schemes mostly aimed to mitigate cross-tier interference between macrocells and residential femtocell networks (RFNs) in which each detached house has one or more FAPs [14-21]. In [14-17], authors proposed channel assignment schemes based on frequency reuse (FR) or fractional frequency reuse (FFR) to assign different channels for macrocell and femtocell networks to improve system performance. However, from performance results, it is shown that even though cross-tier interference is remarkably attenuated, co-tier interference between FAPs significantly increases as the number of FAPs increases. Since then, in [22]-[24], some dynamic channel assignment (DCA) schemes have proposed using efficient heuristic algorithms for in-building dense femtocell networks (DFNs) because the channel assignment considering co-tier interference is a non-linear non-convex NP-Hard problem [25]-[26]. In [26] and [23], authors proposed DCA schemes using graph coloring algorithm (GCA). Each FAP is first included in one FAP cluster in both DCA schemes and subchannels are dynamically assigned to FAP clusters according to the order of maximum capacity of FAP clusters in [26], while using mathematical optimization techniques in [23]. However, even though FAPs have relatively good signal to interference plus noise ratios (SINRs), FAPs use subchannels assigned for one FAP cluster thus the system capacity is limited. On the other hand, in [24], authors proposed a multiple clustering based DCA scheme called graph-based dynamic frequency reuse (GBDFR). In the GB-DFR scheme, each FAP is first included in one FAP cluster by GCA and the same number of subchannels are assigned to FAP clusters. Then, in order to use more subchannels, FAPs find other FAP clusters in which no interfering FAPs are included. However, in the GB-DFR scheme, FAPs are members of as many FAP clusters as possible and it causes that co-tier interference between FAPs to increase significantly. As a result, some FAPs have better performance by using subchannels from more than one FAP cluster while others have worse performance with no additional subchannels and reduced SINRs of femtocell user equipments (FUEs).

In this paper, we propose a novel channel assignment scheme called multi-cluster based dynamic channel assignment (MC-DCA) to improve system performance for the downlink (DL) of DFNs based on orthogonal frequency-division multiple access (OFDMA) and frequency division duplexing (FDD). In order to dynamically assign channels for FAPs, the MC-DCA scheme uses a heuristic method that consists of two steps: one is a multiple

cluster assignment step to group FAPs using GCA with some extensions, while the other is a dynamic subchannel assignment step to allocate subchannels for maximizing the system capacity. Through simulations, we first find optimum parameters of the multiple FAP clustering to maximize the system capacity and then evaluate system performance in terms of the mean FAP capacity, unsatisfied FUE probability, and mean FAP power consumption for data transmission based on a given FUE traffic load. As a result, the MC-DCA scheme outperforms other schemes in two different DFN environments for commercial and office buildings.

The rest of this paper is organized as follows. Section II introduces the system model and problem formulation while Section III describes the proposed MCDCA scheme. Then, simulation results are presented and discussed in Section IV. Finally, Section V concludes this paper with future research direction.

2. System model

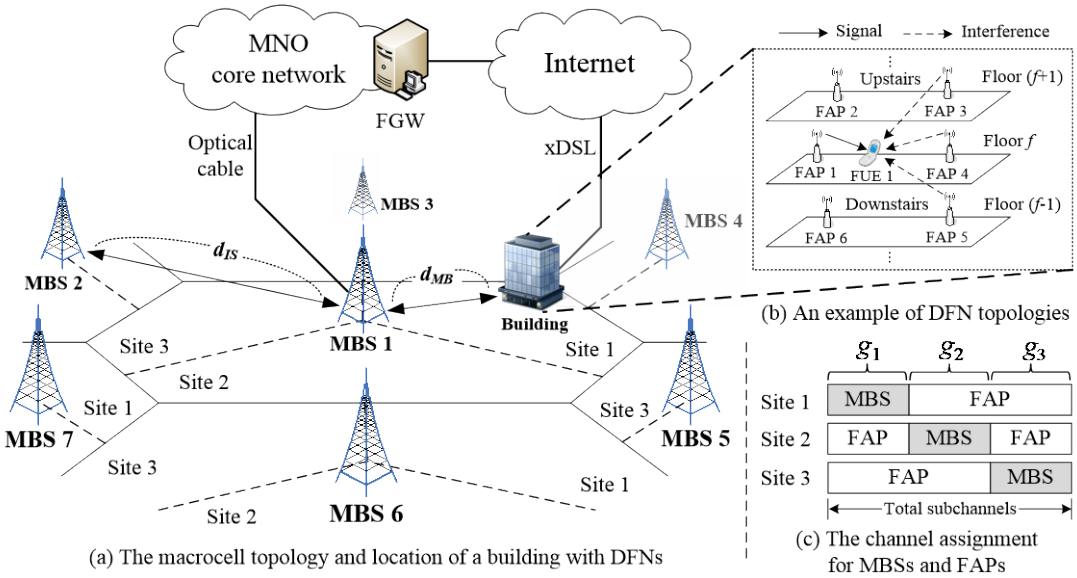

Fig. 1. The system topology and channel assignment: (a) the macrocell topology and location of a building with DFNs, (b) an example of DFN topologies with co-tier interference, (c) the channel assignment for MBSs and FAPs.

2.1 System topology and channel management

We consider a typical two-tier femtocell network architecture where femtocells are overlaped on the macrocell to analyze the system performance of DL DFNs based on OFDMA-FDD. **Fig. 1** shows the system topology and channel management for MBSs and FAPs. There are M hexagonal macrocells and a set of MBSs, $\mathcal{M} = \{1, 2, ..., M\}$ ($M = |\mathcal{M}|$), is installed at the center of each macrocell. We assume that $M = 7$ and the target macrocell is surrounded by six neighbor macrocells as shown in **Fig. 1**-(a). Further, an F-floor building is located in the center macrocell and a set of FAPs, $\mathcal{N} = \{1, 2, ..., N\}$ ($N = |\mathcal{N}|$) composes DFNs in the building. Let d_{IS} and d_{MB} denote the inter-site distance between the center MBS (i.e., MBS 1) and the surrounding MBSs, and between the center MBS and the building with DFNs, respectively. **Fig. 1**-(b) shows an example of DFN topologies in which $\left\lfloor \frac{N}{F} \right\rfloor$ FAPs are uniformly deployed

on each floor of the building and each FAP has not only the co-tier interference coming from the neighbor FAPs in the same floor, but also the co-tier interference coming from the floors above and below. A femtocell gateway (FGW) connected to the DFN controls all FAPs which support no handover request from FUEs (i.e., a centralized management system) while each FAP serves one FUE at a random location in the coverage of the serving FAP with the maximum radius, d_r^{FC}, in meters. In addition, the MBS uses a three-sectored antenna thus the macrocell coverage is divided into three cell sites, site 1, 2, and 3, while the FAP uses an omni-directional antenna. Therefore, MBSs divide total subchannels into three subchannel groups, g_1, g_2, and g_3, to assign for macrocell user equipments (MUEs) in site 1, 2, and 3, respectively, as shown in **Fig. 1**-(c). On the other hand, in order to mitigate cross-tier interference from MBSs, the FGW assigns pairs of two subchannel groups, $g_2 \cup g_3$, $g_1 \cup g_3$, and $g_1 \cup g_2$, which are not used by MBSs but by FAPs in sites 1, 2, and 3, respectively. It is assumed that a set of subchannels, $\mathcal{K}$ = {1, 2, ..., K} ($K = |\mathcal{K}|$), is assigned for FAPs in each site and all FAPs are with open access mode, in which every mobile device in the building can connect to FAPs for mobile services, to focus on analyzing the system performance of DFNs. Finally, we assume perfect knowledge of channel gains, which can be calculated using the propagation losses and shadowing statistics (but ignoring the short-term fading effects).

2.2 Propagation and SINR models

In order to calculate the SINR between the FUE and its serving FAP, we use the ITU indoor path loss model and the COST-231 Hata model (urban area) for indoor and outdoor propagation models, respectively [27][28]. Let L_{in}^{FC} and L_{mn}^{MC} denote path losses of the FUE served by FAP n ($n \in \mathcal{V}$) from FAP i ($i \in \mathcal{V}$) and MBS m ($m \in \mathcal{M}$) in dB, respectively. L_{in}^{FC} and L_{mn}^{MC} can be expressed as

$$L_{in}^{FC} = 20\log_{10}(f_c) + \alpha \log_{10}(d_{in}) + L_f(\delta) - 28 \tag{1}$$

$$\begin{aligned} L_{mn}^{MC} &= 46.3 + 33.9\log_{10}(f_c) + 13.82\log_{10}(h_t) - L_r(h_r) \\ &\quad + (44.9 - 6.55\log_{10}(h_t))\log_{10}(d_{mn}) + 3 + L_w \end{aligned} \tag{2}$$

where f_c is the carrier frequency in MHz, while d_{in} and d_{mn} are distances from the FUE of FAP n to FAP i and to MBS m in meters, respectively. In (1), α and $L_f(\delta)$ are the path loss exponent and the floor loss penetration factor with the number of floors, ($1 \le \delta \le$ F), between the transmitter and receiver [27]. $L_f(\delta)$ can be expressed as

$$L_f(\delta) = \begin{cases} -3(\delta - 1) - 6 & \text{for commercial buildings} \\ -4(\delta - 1) - 15 & \text{for office buildings.} \end{cases} \tag{3}$$

Further, in (2), h_t and h_r denote the antenna heights of MBSs and FUEs in meters, respectively, while $L_r(h_r) = (1.1\log_{10}(f_c) - 0.7)h_r - (1.56\log_{10}(f_c) - 0.8)$ and L_w are the antenna height correction factor of receivers and attenuation loss of an outdoor wall in dB, respectively.

Through (1) and (2), the SINR of the FUE served by FAP n at subchannel k, γ_{nk}, can be expressed as

$$\gamma_{nk} = \frac{p_t^{FC} L_{nn}^{FC} \omega_{nk}}{\sum_{\forall m \in \mathcal{M}} p_t^{MC} L_{mn}^{MC} p_g + \sum_{\forall i \in \mathcal{V} \setminus \{n\}} p_t^{FC} L_{in}^{FC} \omega_{ik} + \sigma_N^2}, \quad \forall n, k, \tag{4}$$

where p_t^{FC} and p_t^{MC} denote the transmission power of each subchannel for the FAP and MBS, respectively. Further, ω_{nk} is an indicator variable in a binary subchannel assignment matrix, $\mathbf{\Omega} = [\omega_{nk}]_{N \times K}$ ($\forall n \in \mathcal{V}, \forall k \in \mathcal{K}$), $\omega_{nk} = 1$ if subchannel k is allocated for FAP n, and 0 otherwise. In addition, σ_N^2 and p_g are the white noise power and the azimuth antenna pattern between MBSs and FUEs in dB, respectively. p_g can be expressed as

$$p_g = \beta_g - \left[12 \left(\frac{\theta}{\theta_{3\text{dB}}} \right)^2, \beta_{\max} \right], \quad -180° \le \theta \le 180°, \tag{5}$$

where β_g and $\beta_{\max}$ are the maximum antenna gain and maximum attenuation in dB, respectively, while θ and $\theta_{3\text{dB}} = 70^\circ$ are the azimuth antenna pattern of MBSs and 3dB beamwidth, respectively [29].

Given a specific γ_{nk} in (4), the spectral efficiency for the FUE of FAP n at subchannel k, r_{nk}, is obtained by

$$r_{nk} = \begin{cases} 0 & \text{if } S_E(\gamma_{nk}) < r_{\min} \\ S_E(\gamma_{nk}) & \text{if } r_{\min} \le S_E(\gamma_{nk}) \le r_{\max} \\ r_{\max} & \text{if } r_{\min} < S_E(\gamma_{nk}), \end{cases} \tag{6}$$

where $S_E(x) = \log_2(1 + \eta x)$ in bps/Hz and $\eta = -1.5 / \ln(5P_e)$ with the target bit error rate P_e [30]. Further, $\gamma_{\min}$ and $\gamma_{\max}$ are the minimum and maximum SINRs in dB, respectively, while $r_{\min} = S_E(\gamma_{\min})$ and $r_{\max} = S_E(\gamma_{\max})$ are the minimum and maximum spectral efficiencies in bps/Hz, respectively [29,31].

2.3 FAP capacity, unsatisfied FUE probability, and power consumption for data transmission

Through (6), the capacity of FAP n, C_n, can be expressed as

$$C_n = W \sum_{\forall k \in \mathcal{K}} \omega_{nk} r_{nk}, \quad \forall n \in \mathcal{V}, \tag{7}$$

where W is the bandwidth of a subchannel in Hz. Further, let the unsatisfied FUE probability, P_{us}, to be the probability that FUEs have capacities less than a given FUE traffic load, ρ, in

bps can be expressed as

$$P_{\text{us}} = \Pr(C_n < \rho), \quad \forall n \in \mathcal{V}. \tag{8}$$

In addition, the power consumption of FAP n, E_n, for data transmission in mW can be expressed as

$$E_n = \sum_{\forall k \in \mathcal{K}} p_t^{FC} \omega_{nk}, \quad \forall n \in \mathcal{V}, \tag{9}$$

3. Multi-cluster based dynamic channel assignment scheme

In this section, we propose the MC-DCA scheme using a heuristic method that consists of two steps, one is a multiple cluster assignment step to group FAPs using GCA with some extensions while the other is a dynamic subchannel assignment step to allocate subchannels.

3.1 Step 1: multiple cluster assignment

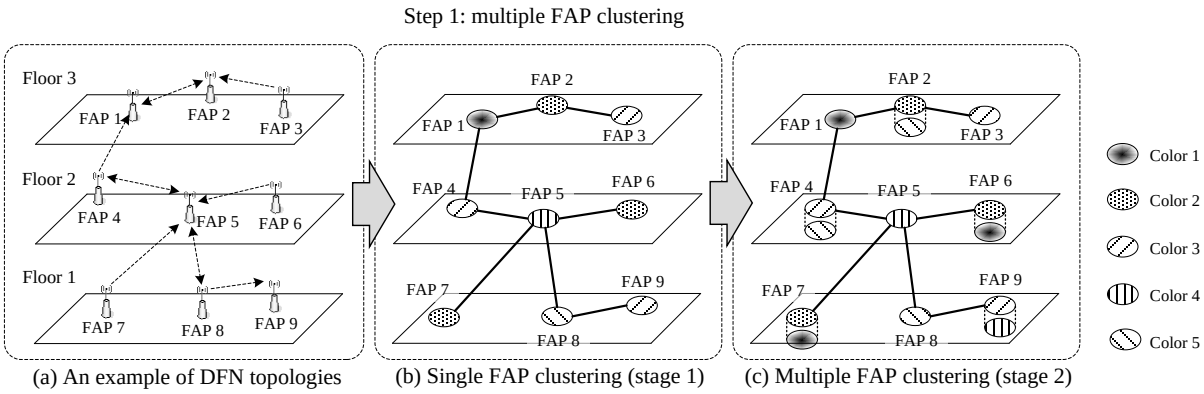

Fig. 2. An example of the multiple FAP clustering step in the MC-DCA scheme: (a) an example of DFN topologies in an F-floor building (F=3, N=9), (b) stage 1: an interference graph using GCA (Y=4), (c) stage 2: multiple FAP clustering based on the interference graph.

Fig. 2 shows an example of the multiple cluster assignment step which has two stages, the FGW first groups FAPs using GCA in stage 1 while adds FAPs to other FAP clusters considering the transmission rate and co-tier interference of FAPs in stage 2. **Fig. 2**-(a) is an example of DFN topologies in which nine FAPs (N = 9) are deployed in a three-floor building (F = 3) and some FAPs have co-tier interference with each other. Under the given DFN topology, in stage 1, the FGW first generates a matrix of ones, $\mathbf{B} = [b_{in}]_{N \times N}$ ($\forall i, n \in \mathcal{V}$), to obtain a binary interference matrix, $\mathbf{J} = [j_{in}]_{N \times N}$ ($\forall i, n \in \mathcal{V}$). Let Γ_n and Γ_{th} be the SINR of the FUE of FAP n calculated by the FGW using received signal strength indicator (RSSI) measurements from FUEs and a given target threshold of the SINR for FUEs ($\gamma_{\min} \le \Gamma_{\text{th}} \le \gamma_{\max}$) in dB, respectively. Γ_n can be obtained by

$$\Gamma_n = \frac{p_t^{FC} L_{nn}^{FC}}{\sum_{\forall m \in \mathcal{M}} p_t^{MC} L_{mn}^{MC} p_g + \sum_{\forall i \in \mathcal{V} \setminus \{n\}} p_t^{FC} L_{in}^{FC} b_{in} + \sigma_N^2} \geq \Gamma_{\text{th}}, \quad \forall n \in \mathcal{V}. \tag{10}$$

Then, the FGW finds an FAP, i_n^*, which gives the strongest co-tier interference to the FUE of FAP n and sets $b_{i_n^* n} = 0$ to avoid co-tier interference if $\Gamma_n < \Gamma_{\text{th}}$ until $\Gamma_n \geq \Gamma_{\text{th}}$. i_n^* can be obtained by

$$i_n^* = \arg \max_{\forall i \in \mathcal{V} \setminus \{n\}} (p_t^{FC} L_{in}^{FC}), \quad b_{in} == 1, \forall n \in \mathcal{V}. \tag{11}$$

After generating $\mathbf{B}$ from (10) and (11), the FGW transforms $\mathbf{B}$ into $\mathbf{J} = \sim \mathbf{B}$ in which "$\sim$" denotes a symbol to convert all elements in $\mathbf{B}$ from 1's to 0's and vice versa. Then, an interference graph $G = (\mathcal{V}, \mathcal{E})$ can be constructed by the FGW using GCA. For the interference graph, $\mathcal{V}$ is used for the vertex set while $\mathcal{E}$ is the edge set to denote co-tier interference between FAPs in $\mathbf{J}$. Further, no two connected vertices in $\mathcal{E}$ have the same color, that is, the color means the FAP cluster and interfering FAPs do not become members of the same FAP cluster. For the GCA, we use DSATUR (Degree of Saturation) algorithm in which a predetermined order based on the number of different colors adjacent to the vertex, called the saturation degree of a vertex, is used to color the vertices [32]. Finally, from the interference graph, the FGW obtains a minimum number of colors, $Y = |\mathcal{Y}|$, $\mathcal{Y} = \{1, 2, ..., Y\}$, and generates a binary FAP cluster matrix, $\mathbf{Z} = [z_{ny}]_{N \times Y}$ ($\forall n \in \mathcal{V}, \forall y \in \mathcal{Y}$). z_{ny} can be obtained by

$$z_{ny} = \begin{cases} 1 & \text{If color y is assigned to the FUE of FAP } n \\ 0 & \text{otherwise.} \end{cases} \tag{12}$$

In addition, in order to add FAPs to other FAP clusters in stage 2, the FGW finds available FAP clusters for FUEs and generates a binary available FAP cluster matrix, $\mathbf{A} = [a_{ny}]_{N \times Y}$ ($\forall n \in \mathcal{V}, \forall y \in \mathcal{Y}$), considering co-tier interference based on $\mathbf{J}$. a_{ny} can be obtained by

$$a_{ny} = \begin{cases} 1 & \text{If } z_{ny} == 1 \text{ and } j_{in} == 0, \quad \forall i \in \mathcal{V} \setminus \{n\} \\ 0 & \text{otherwise.} \end{cases} \tag{13}$$

In **Fig. 2**-(b), for example, the FGW generates an interference graph with four different colors (Y=4) using GCA, and FAPs which have the same colors become members of the same FAP clusters. Then, the FGW finds available FAP clusters for each FAP considering co-tier interference in $\mathbf{J}$, that is, FAP 1, 2, and 3 become members of FAP cluster 4, FAP 4 and 6 become members of FAP cluster 2, and so on.

Using $\mathbf{Z}$ and $\mathbf{A}$, in stage 2, the FGW adds FAPs to other FAP clusters and FAPs that are members of additional FAP clusters use more subchannels. The FGW first finds an FAP, n^*, which has available clusters in $\mathbf{A}$ with minimum $S_E(\Gamma_n)$ ($\forall n \in \mathcal{V}$), to give higher priority, to be added into additional FAP clusters. n^* can be obtained by

$$n^* = \arg\max_{\forall n \in \mathcal{V}} \left(\sum_{\forall y \in \mathcal{Y}} S_E(\Gamma_n) z_{ny} \right). \tag{14}$$

Also, the FGW finds an available cluster, y^*, which offers maximum $S_E(\Gamma_{n^*})$ for FAP n^* in $\mathbf{A}$. y^* can be obtained by

$$y^* = \arg\max_{\forall y \in \mathcal{Y}} \left(S_E(\Gamma_{n^*}) a_{n^* y} \right). \tag{15}$$

In **Fig. 2**-(c), for example, the FGW adds some FAPs which have available FAP clusters and higher priority, to other FAP clusters. It is assumed that the order of priority to add FAP clusters obtained by (15) is from (i) to (ix). Therefore, FAP 2 is first added to FAP cluster 4 while FAP 1 and 3 have no chance to be added to FAP cluster 4 because of the co-tier interference with FAP 2. Then, both FAP 4 and 6 are added to FAP cluster 2, while FAP 5 has no available FAP clusters. Furthermore, FAP 7 is added to FAP cluster 3, while FAP 8 has no chance. Finally, FAP 9 is added to both FAP cluster 1 and 3. The procedure of the multiple FAP clustering step is described in Algorithm 1. In order to decide the addition of FAPs to other FAP clusters, the FGW first calculates the total spectral efficiency of FAPs in cluster y^*, R_1, in line 16 and then once again computes it, R_2, after adding FAP n^* in line 18. As a result, if $R_1 < R_2$ and $\Gamma_n \geq \gamma_{\min}$ ($\forall n \in y^*$), the FGW adds FAP n^* to FAP cluster y^* as well as setting $a_{iy^*} = 0$ to avoid co-tier interference in line 20. Otherwise, it does not add FAP n^* by setting $z_{n^* y^*} = 0$ in line 22.

Algorithm 1 : Multiple cluster assignment (step 1)

Input: $\mathcal{V}$, Γ_{th}, L_{in}^{FC}, L_{mn}^{MC}, $\forall i,n \in \mathcal{V}$, $\forall m \in \mathcal{M}$.

Output: $\mathbf{Z}$.

Initialization: z_{ny}, a_{ny}, $b_{in} = 0$, $j_{in} = 1$, $\forall i,n \in \mathcal{V}$, $\forall y \in \mathcal{Y}$.

1: // Stage 1: group FAPs using GCA from line 2 to 12.
2: **for** *n*=1 to *N* **do**
3: Calculate Γ_n according to (11);
4: **while** $\Gamma_{\text{th}} > \Gamma_n$ **do**
5: Find i_n^* according to (12);
6: Set $b_{i_n^* n} = 0$ in $\mathbf{B}$; // Add interfering FAPs
7: Calculate Γ_n according to (11);
8: **end while**
9: **end for**
10: Create an interference graph using GCA with $\mathbf{J} = \sim \mathbf{B}$;
11: Obtain $\mathcal{Y}$ from the interference graph;
12: Generate $\mathbf{Z}$ and $\mathbf{A}$ according to (13) and (14), respectively;
13: // Stage 2: add FAPs to other clusters from line 14 to 24.
14: **while** $\mathbf{A} \neq \emptyset$ **do**

15: Find n^* and y^* according to (15) and (16), respectively;
16: $R_1 = \sum_{\forall n \in \mathcal{V}} S_E(\Gamma_n) z_{ny^*}$;
17: Set $z_{n^*y^*} = 1$ and $a_{n^*y^*} = 0$;
18: $R_2 = \sum_{\forall n \in \mathcal{V}} S_E(\Gamma_n) z_{ny^*}$;
19: **if** $R_1 < R_2$ **and** $\Gamma_n \geq \gamma_{\min} (\forall n \in y^*)$ **then**
20: Set $a_{iy^*} = 0$ if $a_{iy^*} == 1$ and $j_{in^*} == 1$, $\forall i \in \mathcal{V} \setminus \{n^*\}$;
21: **else**
22: Set $z_{n^*y^*} = 0$; // The FGW decides not to add FAPs
23: **end if**
24: **end while**

3.2 Step 2: dynamic subchannel assignment

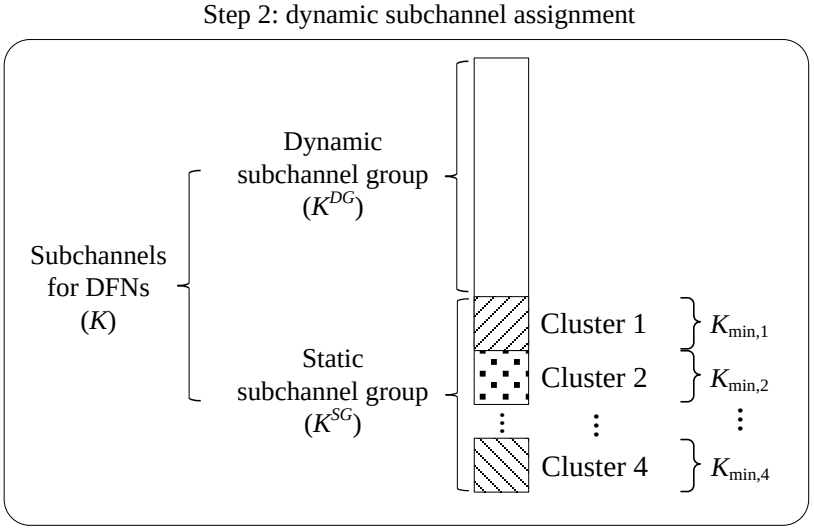

Fig. 3. An example of the dynamic subchannel assignment step with four FAP clusters ($Y = 4$) in the MC-DCA scheme.

In step 2, the FGW dynamically assigns subchannels in $\mathcal{K}$ to FAPs based on ρ and $\mathbf{Z}$ obtained by step 1. In order to guarantee the minimum number of subchannels for each FAP, $K_{\min} = |\mathcal{K}_{\min,y}|$ ($\forall y \in \mathcal{Y}$), the FGW first divides $\mathcal{K}$ into two subchannel groups named static subchannel group and dynamic subchannel group, $\mathcal{K}^{SG}$ and $\mathcal{K}^{DG}$, as shown in **Fig. 3**. $\mathcal{K}^{SG}$ and $\mathcal{K}^{DG}$ can be obtained by

$$\mathcal{K}^{SG} = \bigcup_{\forall y \in \mathcal{Y}} \mathcal{K}_{\min,y}, \quad \mathcal{K}^{DG} = \mathcal{K} - \mathcal{K}^{SG}. \tag{16}$$

In **Fig. 3**, for example, the FGW has four FAP clusters (Y = 4) thus $|\mathcal{K}^{SG}| = YK_{\min} = 4K_{\min}$. After assigning subchannels in $\mathcal{K}^{SG}$ to FAPs, some FAPs included in one FAP cluster have $K_{\min}$ subchannels while others in multiple FAP clusters have more than $K_{\min}$ subchannels. Then, the FGW finds a cluster, y^{**}, with maximum spectral efficiency of FAP clusters, to maximize the mean FAP capacity and dynamically assigns subchannel k ($\forall k \in \mathcal{K}^{DG}$) to FAPs. y^{**} can be obtained by

$$y^{**} = \arg\max_{\forall y \in \mathcal{Y}} \left(\sum_{\forall n \in \mathcal{V}} S_E(\Gamma_n) z_{ny} \right), \quad \forall k \in \mathcal{K}^{DG}. \tag{17}$$

Using (17) and (18), the FGW assigns subchannel k to FAP n by setting $\omega_{nk} = 1$ in $\mathbf{\Omega}$ ($\forall n \in \mathcal{V}, \forall k \in \mathcal{K}$). The procedure of dynamic subchannel assignment step is described in Algorithm 2. Meanwhile, some FAPs become satisfied with ρ before all subchannels in $\mathcal{K}^{DG}$ are assigned. Therefore, in order to efficiently assign subchannels, the FGW dynamically sets $C_n = \rho$ and $z_{ny} = 0$ ($\forall n \in \mathcal{V}, \forall y \in \mathcal{Y}$) in line 7 and 16 if $C_n \geq \rho$.

Algorithm 2 : Dynamic subchannel assignment (step 2)

Input: $\mathcal{K}$, $\mathcal{V}$, $\mathcal{Y}$, $\mathbf{Z}$.
Output: $\mathbf{\Omega}$.
Initialization: $\omega_{nk} = 0$, $\forall n \in \mathcal{V}$, $\forall k \in \mathcal{K}$.
1: Divide $\mathcal{K}$ into $\mathcal{K}^{SG}$ and $\mathcal{K}^{DG}$ according to (17).
2: // Assign subchannels in $\mathcal{K}^{SG}$ from line 3 to 9.
3: **for** y = 1 to Y **do**
4: $\omega_{nk} = 1$, if $z_{ny} == 1$ ($\forall n \in \mathcal{V}, \forall k \in \mathcal{K}_{\min,y}$);
5: Calculate C_n ($\forall n \in \mathcal{V}, z_{ny} == 1$) according to (7);
6: **if** $C_n \geq \rho$ ($\forall n \in \mathcal{V}, z_{ny} == 1$) **then**
7: Set $C_n = \rho$ and $z_{ny} = 0$ ($\forall y \in \mathcal{Y}$);
8: **end if**
9: **end for**
10: // Assign subchannels in $\mathcal{K}^{DG}$ from line 11 to 18.
11: **for** k = 1 to $|\mathcal{K}^{DG}|$ **do**
12: Find y^{**} according to (18);
13: $\omega_{nk} = 1$, if $z_{ny} == 1$ ($\forall n \in \mathcal{V}$);
14: Calculate C_n ($\forall n \in \mathcal{V}, z_{ny} == 1$) according to (7);
15: **if** $C_n \geq \rho$ ($\forall n \in \mathcal{V}, z_{ny} == 1$) **then**
16: Set $C_n = \rho$ and $z_{ny} = 0$ ($\forall y \in \mathcal{Y}$);
17: **end if**
18: **end for**

4. Simulation results and discussions

In this section, we investigate the performance of the MC-DCA scheme in terms of the mean FAP capacity, unsatisfied FUE probability, and mean FAP power consumption for data transmission using a Monte Carlo simulation. In order to demonstrate superiority, we compare the MC-DCA scheme to four different schemes: dynamic clustering based subband allocation (DCSA) [22], GB-DFR [24], graph based static channel assignment (GB-SCA), and frequency reuse 1 (FR 1). In the GB-SCA scheme, the FGW first groups FAPs using GCA (i.e., stage 1 in subsection 3.1) and assigns subchannels for each FAP cluster, while in the FR 1 scheme every FAP uses all subchannels in $\mathcal{K}$ without considering co-tier interference. The system topology and channel assignment for MBSs and FAPs are as shown in **Fig. 1**. Further, it is assumed that the building with DFNs has five floors (F=5), thus, for example, 20 FAPs are randomly deployed on each floor when N=100. Log-normal shadow fading is considered with zero mean and standard deviation of 4dB and 10dB for macrocell and femtocell networks, respectively [28]. The system parameters are listed in **Table 1**.

Table 1. System parameters.

Parameter	Value
Carrier frequency (f_c)	2GHz
Total bandwidth	4.5MHz
Bandwidth per subchannel (W)	5KHz
The numbers of total subchannels, subchannels for MBSs and FAPs/cell site	900, 300, 600
The number of floors/building (F)	5
The number of FAPs/building (N)	20, 40, 60, 80, 100
FUE traffic load (ρ)	1 and 1.5Mbps
The number of FUEs/FAP	1
The inter-site distance between MBSs (d_{IS})	1km
FAP radius (d_r^{FC})	5m
Distance between the building and MBS (d_{ME})	400m
The area of the building	50m x 50m
The height of each floor in the building	3m
The height of MBSs	25m
The height of FAPs (h_t) and FUEs (h_r)	1.5 and 1m
Min distance between FAPs	3m
Min distance between the FAP and FUE	0.2m [29]
MBS's total transmission power	20W [29]
FAP's total transmission power	10mW [29]
α for commercial and business buildings	22, 30 [27]
Min number of subchannels ($K_{\min}$)	10
Min and Max SINRs ($\gamma_{\min}, \gamma_{\max}$)	-10dB, 18.5dB [31]
Min and Max spectral efficiencies ($r_{\min}, r_{\max}$)	0.137, 4.4bps/Hz [31]
Bit error rate (P_e)	10^{-3} [30]
The maximum antenna gain (β_g) and maximum attenuation ($\beta_{\max}$)	14dB, 20dB [29]
Standard deviation for the MBS and FAP	4dB, 10dB [29]
σ_N^2	-174dBm/Hz

In addition, we consider two in-building DFN environments using α =22 and 30 for commercial and office buildings, respectively, since the system performance is greatly influenced by the indoor environments [23]. That is, the commercial building has more open space inside compared to that of the office building, thus FAPs have more serious co-tier interference in commercial buildings.

4.1 Commercial buildings

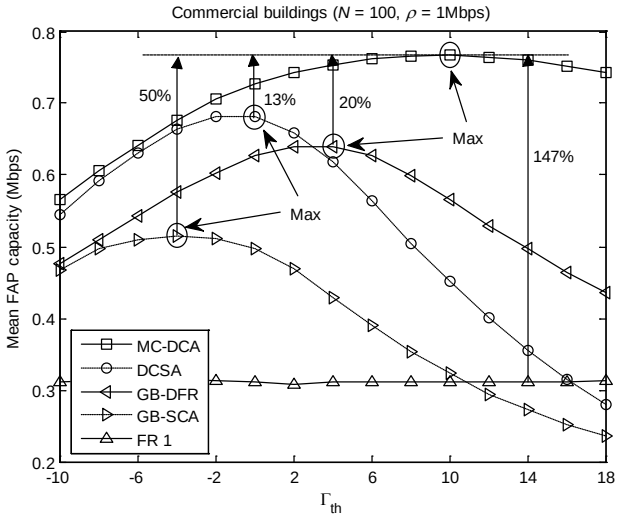

Fig. 4. Mean FUE capacity vs. Γ_{th} in commercial buildings.

Fig. 4 describes the results of the mean FAP capacity in commercial buildings as Γ_{th} increases when N = 100 and ρ = 1Mbps. The MC-DCA, DCSA, GB-DFR, and GB-SCA schemes show convex graphs because the SINR of FUEs increases but the number of subchannels per FAP cluster decreases (since Y increases) as Γ_{th} increases. In other words, FAPs use more subchannels with lower SINRs of FUEs when Γ_{th} is low, and use less subchannels with higher SINRs of FUEs when Γ_{th} is high. Therefore, it is shown that the optimum values of Γ_{th} with maximum mean FAP capacities are 10, 0, 4, and -4dB for the MC-DCA, DCSA, GB-DFR, and GB-SCA schemes, respectively. As a result, based on the optimum values of Γ_{th}, the MC-DCA scheme outperforms others and is 13, 20, 50, and 147% better than the DCSA, GB-DFR, GB-SCA, and FR 1 schemes, respectively. Further, even though FAPs have one FAP cluster, the DCSA scheme has better performance than the GB-DFR scheme. This is because the DCSA scheme has lower interference between FAPs and dynamically assigns subchannels to FAP clusters according to the order of maximum capacity of FAP clusters. The GB-DFR scheme shows higher performance than the DCSA scheme using more subchannels with increased SINRs of FUEs when $\Gamma_{th} \geq$ 3dB but the maximum mean FAP capacity is still lower. Then, the GB-DFR scheme has higher performance than the GB-SCA scheme since it assigns FAPs to multiple FAP clusters to use more subchannels. Finally, the FR 1 scheme has the worst performance with strong co-tier interference and is not affected by Γ_{th} thus the result is always the same at 0.32Mbps.

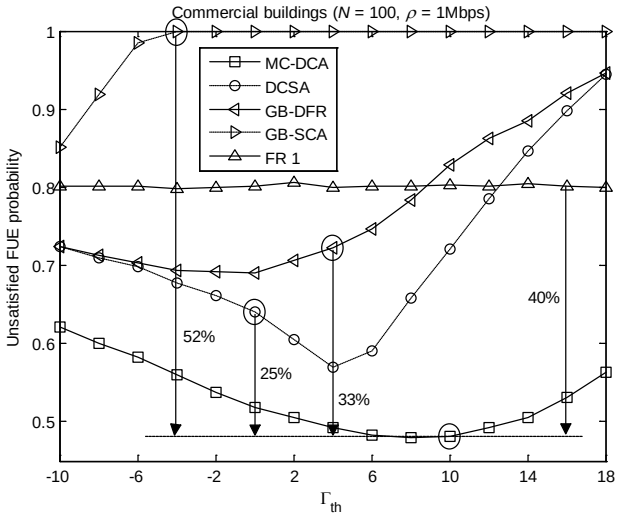

Fig. 5. Unsatisfied FUE probability vs. Γ_{th} in commercial buildings.

Fig. 5 depicts the results of unsatisfied FUE probability in commercial buildings as Γ_{th} increases when N = 100 and ρ = 1Mbps. The MC-DCA, DCSA, and GBDFR schemes show concave graphs while the GB-SCA scheme becomes 1 when $\Gamma_{th} \geq -4$dB since all FAPs have an insufficient number of subchannels for each FAP cluster. The FR 1 scheme performs better than the GB-SCA scheme. Based on the optimum values of Γ_{th} obtained in **Fig. 4**, it is shown that the unsatisfied FUE probability of the MC-DCA scheme is 25, 33, 52, and 40% lower than the DCSA, GB-DFR, GB-SCA, and FR 1 schemes, respectively.

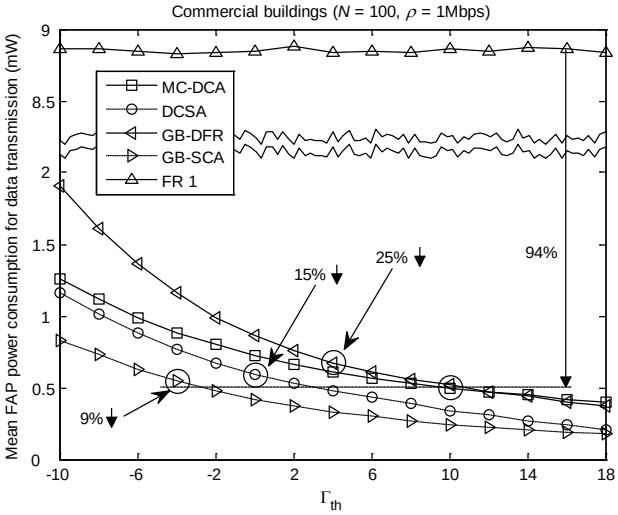

Fig. 6. Mean FAP power consumption for data transmission vs. Γ_{th} in commercial buildings.

Fig. 6 shows the results of mean FAP power consumption for data transmission in commercial buildings as Γ_{th} increases when N = 100 and ρ = 1Mbps. The FR 1 scheme has approximately 0.88mW and is much higher than others while the MC-DCA, DCSA, GB-DFR, and GB-SCA schemes reduce as Γ_{th} increases. The MC-DCA and GB-DFR schemes assign

FAPs to multiple FAP clusters to use more subchannels thus show higher power consumption than the DCSA and GBSCA schemes. However, based on the optimum values of Γ_{th} obtained in **Fig. 4**, the MC-DCA scheme outperforms others and reduces the power consumption by about 15, 25, 9, and 94% compared to the DCSA, GB-DFR, GB-SCA, and FR 1 schemes, respectively. Meanwhile, the GB-DFR scheme adds FAPs to available FAP clusters and thus shows a higher power consumption compared to the MCDCA scheme but the MC-DCA scheme becomes higher when $\Gamma_{th} \geq 12$dB. This is because the MC-DCA scheme assigns subchannels according to the order of maximum spectral efficiency of FAP clusters, thus more FAPs with higher SINRs of FUEs use subchannels while the GB-DFR scheme assigns the same number of subchannels per FAP cluster, thus FAPs with higher SINRs of FUEs remain subchannels in multiple FAP clusters but with lower SINRs of FUEs still need more subchannels.

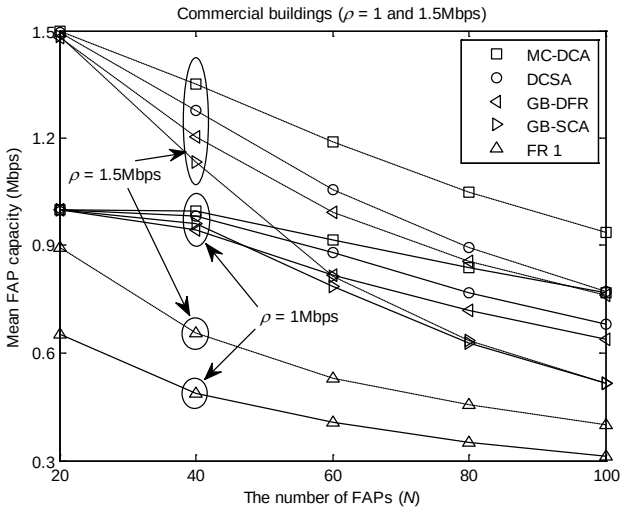

Fig. 7. Mean FAP capacity vs. the number of FAPs in commercial buildings: ρ =1Mbps (solid line) and 1.5Mbps (dotted line).

Fig. 7 describes the results of the mean FAP capacity in commercial buildings as N increases when ρ = 1 and 1.5Mbps (solid and dotted lines). We first found the optimum values of Γ_{th} according to different *N* and ρ as shown in Table 2 and then used them for performance evaluation. The MC-DCA, DCSA, GB-DFR, and GB-SCA schemes have almost the same performance when *N*=20 because of low co-tier interference. On the other hand, the MC-DCA scheme shows better performance than others in both ρ = 1 and 1.5Mbps when $N > 20$ and the gap of capacities between the MC-DCA and other schemes is increasingly bigger as *N* increases. As a result, FAPs are greatly influenced by co-tier interference from neighbor FAPs and the performance decreases significantly as *N* increases in commercial buildings.

4.2 Office buildings

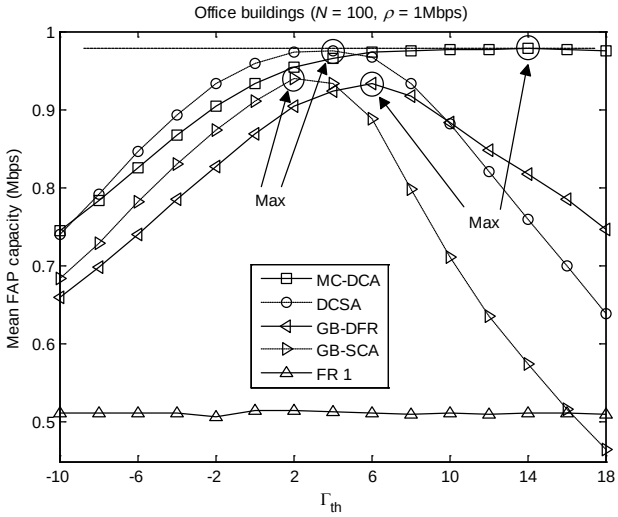

Fig. 8. Mean FUE capacity vs. Γ_{th} in office buildings.

Fig. 8 describes the results of the mean FAP capacity in office buildings as Γ_{th} increases when N = 100 and ρ = 1Mbps. The DCSA, GB-DFR, and GB-SCA schemes show convex graphs while the MC-DCA scheme does not decrease when Γ_{th} > 6dB. This is because the MC-DCA scheme uses more subchannels without strong co-tier interference in office buildings. Therefore, it is shown that the optimum values of Γ_{th} with maximum mean FAP capacities are 14, 4, 6, and 2dB for the MC-DCA, DCSA, GB-DFR, and GB-SCA schemes, respectively. As a result, based on the optimum values of Γ_{th}, the MC-DCA scheme outperforms others and is 0.2, 5, 4, and 90% better than the DCSA, GB-DFR, GB-SCA, and FR 1 schemes, respectively. Meanwhile, the FR 1 scheme consistently shows the same capacity at 0.52Mbps.

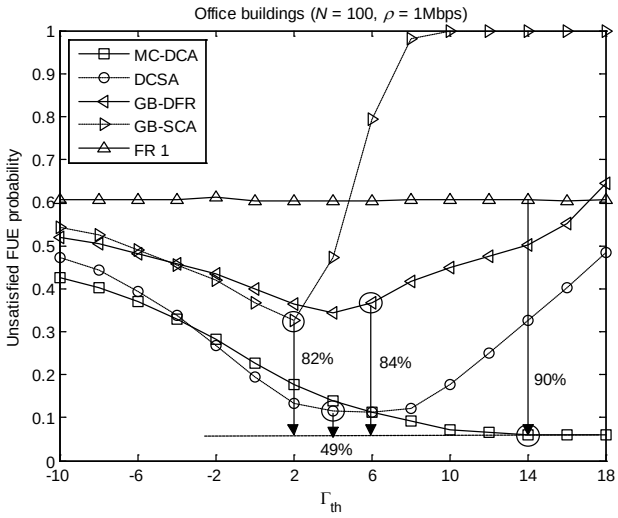

Fig. 9. Unsatisfied FUE probability vs. Γ_{th} in office buildings.

Fig. 9 depicts the results of unsatisfied FUE probability in office buildings as Γ_{th} increases when N = 100 and ρ = 1Mbps. The DCSA, GB-DFR, and GBSCA schemes show concave graphs while the GB-SCA scheme becomes 1 when $\Gamma_{th} \geq$ 10dB. Further, the MC-DCA scheme shows similar results when $\Gamma_{th} \geq$ 14dB while the FR 1 scheme continuously has the same Pus at approximately 0.61. As a result, based on the optimum values of Γ_{th} obtained in **Fig. 8**, the unsatisfied FUE probability of the MC-DCA scheme is 49, 84, 82, and 90% lower than the DCSA, GB-DFR, GB-SCA, and FR 1 schemes, respectively.

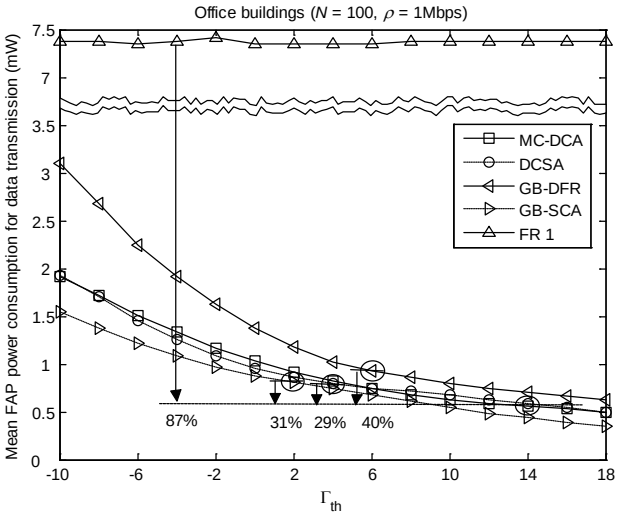

Fig. 10. Mean FAP power consumption for data transmission vs. Γ_{th} in office buildings.

Fig. 10 shows the results of mean FAP power consumption for data transmission in office buildings as Γ_{th} increases when N = 100 and ρ = 1Mbps. The FR 1 scheme has approximately 0.74mW and is much higher than others while the MC-DCA, DCSA, GB-DFR, and GB-SCA schemes reduce as Γ_{th} increases. Based on the optimum values of Γ_{th} obtained in **Fig. 8**, the MC-DCA scheme reduces the power consumption by about 29, 40, 31, and 87% compared to the DCSA, GB-DFR, GB-SCA, and FR 1 schemes, respectively.

Fig. 11 describes the results of the mean FAP capacity in office buildings as N increases when ρ = 1 and 1.5Mbps (solid and dotted lines). We use the optimum values of Γ_{th} as shown in Table 2 for performance evaluation. The MC-DCA, DCSA, GB-DFR, and GB-SCA schemes have almost the same performance when ρ = 1Mbps while the MC-DCA scheme outperforms others when ρ = 1.5Mbps. As a result, in office buildings, FAPs have less co-tier interference compared to commercial buildings thus the mean FAP capacity of the MC-DCA, DCSA, GBDFR, and GB-SCA schemes is close to 1Mbps until $N \leq 80$ when ρ = 1Mbps, while is reduced from $40 \leq N$ when ρ = 1.5Mbps. Meanwhile, the FR 1 scheme is much lower than other schemes and reduces from $20 \leq N$.

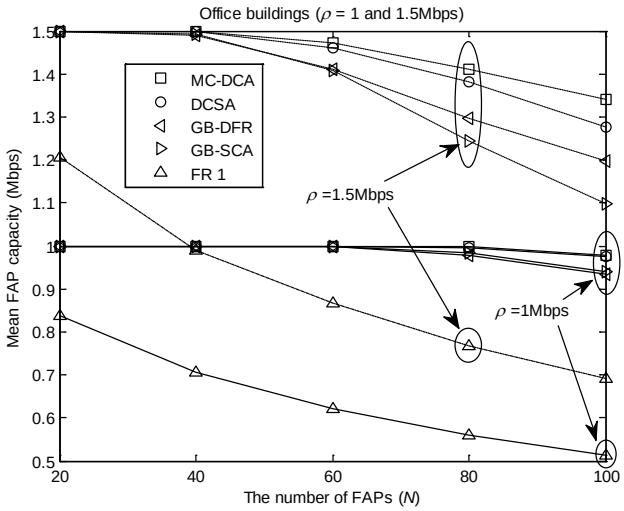

Fig. 11. Mean FAP capacity vs. the number of FAPs in office buildings: ρ =1Mbps (solid line) and 1.5Mbps (dotted line).

5. Conclusions

In this paper, we proposed a novel dynamic channel assignment scheme called MC-DCA to improve system performance for DL DFNs based on OFDMA and investigated the MC-DCA scheme compared to the DCSA, GB-DFR, GB-SCA, and FR 1 schemes. Further, we considered two different DFN environments for commercial and office buildings in which FAPs have different co-tier interference effects with each other. Through simulations, we first found the optimum values of Γ_{th} to maximize the system capacity and then evaluated system performance in terms of the mean FAP capacity, unsatisfied FUE probability, and mean FAP power consumption for data transmission according to different parameters, N and ρ. Simulation results showed that the MC-DCA scheme has better performance for not only the mean FAP capacity and unsatisfied FUE probability but also the FAP power consumption for data transmission. For future work, we are planning to study a multiple cluster based DCA scheme with adaptive power control for data transmission to improve system performance of DFNs.

References

[1] Release one: Home-overview, Small Cell Forum, 2013. Article (CrossRef Link).
[2] Cisco Visual Networking Index: Forecast and Methodology, 2012-2017, White paper, CISCO, 2013. Article (CrossRef Link).
[3] 3GPP TS 22.220, Service Requirements for Home NodeB (HNB) and Home eNodeB (HeNB), 2009. Article (CrossRef Link).
[4] 3GPP TR 23.830, Architecture Aspects of Home NodeB and Home eNodeB, 2009. Article (CrossRef Link).
[5] Chandrasekhar, V., Andrews, J., Gatherer, A., "Femtocell Networks: A Survey," *IEEE Communications Magazine*, vol.46. no.9, pp.59-67, 2008. Article (CrossRef Link).
[6] Hanchate, S., Borsune, S., Shahapure, S., "3GPP LTE Femtocell - Pros & Cons", *International Journal of Engineering Science & Advanced Technology*, vol.2, no.6, pp.1596-1602, 2012. Article (CrossRef Link).

[7] Knisely, D., Yoshizawa, T., Favichia, F., "Standardization of femtocells in 3GPP," *IEEE Communications magazine*, vol.47, no.9, pp.68-75, 2009. Article (CrossRef Link).
[8] Golaup, A., Mustapha, M., Patanapongpibul, L., "Femtocell Access Control Strategy in UMTS and LTE", *IEEE Communications Magazine*, vol.47, no.9, pp.117-123, 2009. Article (CrossRef Link).
[9] Hassan, W. A., Jo, H.-S., and Rahman, T. A., "Simulation Model for Compatibility between LTE-Advanced and Digital Broadcasting in the Digital Dividend Band," *Smart Computing Review*, vol.3, no.5, pp.309-322, 2013. Article (CrossRef Link).
[10] Kim, R., Kwak, J., Etemad, K., "WiMAX femtocell: requirements, challenges, and solutions," *IEEE Communications Magazine*, vol.47, no.9, pp.84-91, 2009. Article (CrossRef Link).
[11] Li, Y., Maeder, A., Fan, L., Nigam, A., Chou, J., "Overview of femtocell support in advanced WiMAX systems," *IEEE Communications Magazine*, vol.49, no.7, pp.122-130, 2011. Article (CrossRef Link).
[12] Zahir, T., Arshad, K., Nakata, A., Moessner, K., "Interference management in femtocells," *IEEE Communications Surveys & Tutorials*, vol.15, no.1, pp.293-311, 2013. Article (CrossRef Link).
[13] Lopez-Perez, D., Valcarce, A., de la Roche, G., Zhang J., "OFDMA femtocells: A roadmap on interference avoidance", *IEEE Communications Magazine*, vol.47, no.9, pp.41-48, 2009. Article (CrossRef Link).
[14] Lee, H., Oh, D., Lee, Y., "Mitigation of Inter-Femtocell Interference with Adaptive Fractional Frequency Reuse", *in Proc. of IEEE ICC*, 2010. Article (CrossRef Link).
[15] Chowdhury, M., ang, Y., Haas, Z., "Cost-Effective Frequency Planning for Capacity Enhancement of Femtocellular Networks," *Wireless Personal Communications*, vol.60, no.1, pp.83-104, 2011. Article (CrossRef Link).
[16] Saquib, N., Hossain, E., Le, L., Kim, D., "Interference Management in OFDMA Femtocell Networks: Issues and Approaches," *IEEE Wireless Communications*, vol.19, no.3, pp.86-95, 2012. Article (CrossRef Link).
[17] Oh, C., Chung, M., Choo, H., Lee, T., "Resource Allocation with Partitioning Criterion for Macro-Femto Overlay Cellular Networks with Fractional Frequency Reuse," *Wireless Personal Communications*, vol.68, no.2, pp.417-432, 2013. Article (CrossRef Link).
[18] Zhang, H., Jiang, C., Beaulieu, N., Chu, X., Wen, X., and Tao, M., "Resource Allocation in Spectrum-Sharing OFDMA Femtocells with Heterogeneous Services," *IEEE Transactions on Communications*, vol.62, no.7, pp.2366-2377, 2014. Article (CrossRef Link).
[19] Zhang, H., Jiang, C., Beaulieu, N. C., Chu, X., Wang, X., and Quek, T. Q. S., "Resource Allocation for Cognitive Small Cell Networks: A Cooperative Bargaining Game Theoretic Approach," *IEEE Transactions on Wireless Communications*, vol.14, no.6, pp.3481-3493, 2015. Article (CrossRef Link).
[20] Zhang, H., Jiang, C., Mao, X., Chen, H., "Interference-Limited Resource Optimization in Cognitive Femtocells with Fairness and Imperfect Spectrum Sensing," *IEEE Transactions on Vehicular Technology*, vol-, no.99, pp.1-1, 2015. Article (CrossRef Link).
[21] Maksymyuk, T., Brych, M, Strykhalyuk, I., and Jo, M., "Fractal Modeling for Multi-Tier Heterogeneous Networks with Ultra-High Capacity Demands," *Smart Computing Review*, vol.5, no.3, pp.346-355, 2015. Article (CrossRef Link).
[22] Li, W., Su, T., Gheng, W., Wen, X., "Clustering Based Resource Allocation for Inter-femtocell Interference Management", *Journal of Computational Information Systems*, vol.8, no.4, pp.1457-1466, 2012. Article (CrossRef Link).
[23] Zheng, K., Wang, Y., Lin, C., Shen, X., Wang, J., "Graph-based interference coordination scheme in orthogonal frequency-division multiplexing access femtocell networks," *IET Communications*, vol.5, no.17, pp.2533-2541, 2011. Article (CrossRef Link).
[24] Uygungelen, S., Auer, G., Bharucha, Z., "Graph-Based Dynamic Frequency Reuse in Femtocell Networks," in *Proc. of IEEE VTC Spring*, 2011. Article (CrossRef Link).
[25] Chiang, M., "Geometric Programming for Communications Systems," *Foundations Trends Commun. Inf. Theor.*, vol.2, no.2, pp.1-156, 2005. Article (CrossRef Link).
[26] Zhang, T., Multi-stage Convex Relaxation for Non-convex Optimization, Technical report,

Rutgers Tech Report, 2009. Article (CrossRef Link).
[27] Recom. ITU-R P.1238-6, Propagation data and prediction methods for the planning of indoor radiocommunication systems and radio local area networks in the frequency range 900 MHz to 100 GHz, 2009. Article (CrossRef Link)3
[28] COST 231 Final report, European Cooperation in the Field of Scientific and Technical Research, Digital Mobile Radio Towards Future Generation Systems. Article (CrossRef Link).
[29] 3GPP TSG-RAN WG 4, R4-092042, Simulation assumptions and parameters for FDD HeNB RF requirements, 2009. Article (CrossRef Link).
[30] Qiu, X. and Chawla, K., "On the performance of adaptive modulation in cellular systems," *IEEE Communications*, vol.47, no.6, pp.884-895, 1999. Article (CrossRef Link).
[31] 3GPP TR 36.942 V11.0.0, Evolved Universal Terrestrial Radio Access (E-UTRA); Radio Frequency (RF) System Scenarios, 2009. Article (CrossRef Link).
[32] Brelaz, D., "New methods to color the vertices of a graph," *Communications of the ACM*, Machinery 22, pp.251-256, 1979. Article (CrossRef Link).

Se-Jin Kim received the B.S. degree from the Department of Computer Science at Chosun University, Gwangju, Korea, in 2004, and M.S. and Ph.D. degrees from the Department of Computer Science at Korea University, Seoul, Korea, in 2006 and 2010, respectively. He was a post-doctoral fellow in the Department of Electrical Engineering at University of Washington, Seattle, USA and the Department of Electrical and Computer Engineering at University of British Columbia, Vancouver, Canada in 2012 and 2013-2014, respectively. He is an assistant professor in the Department of Computer Science and Statistics at Chosun University, Gwangju, Korea.

IlKwon Cho received the B.S. and M.S. degrees from the in Department of Electronic Engineering at Hanyang University, Seoul, Korea, in 1996 and 1998, respectively. He received Dr. degree of communication engineering at Kyushu University, Japan in Jan. 2010. He started his work in LG cable co. from 1998. Since 2003, he has been in National Information society Agency (NIA), Seoul, Korea, as a executive principal researcher. He is currently a member of associate editor of Human-centric Computing and Information Sciences, and technical committee of International Academy, Research, and Industry Association (IARIA) Journal. His research interests include Internet and network architecture, traffic steering, measurement, modeling, and analysis. He is currently interested in femtocell networks, mobility management and SDN/NFV enabled mobile networks.

ByungBog Lee received his B.S., M.S. and Ph.D. degrees in Computer Science from Howon University, Chonbuk National University and Korea University in 1991, 1993 and 2010, respectively. He is currently a principal researcher at the Electronics and Telecommunications Research Institute, Korea. His current research interests include mobile communications, sensor networks, machine-to-machine networks, and Internet-of-Things networks. He is currently doing researches into the smartphone-based thing personalization schemes and thing finder/browser for Internet-of-Things networks.

Sang-Hyun Bae received the B.S. and M.S. degrees from the Department of Electrical Engineering at Chosun University, Gwangju, Korea, in 1982 and 1984, and Ph.D. degree from the Department of Information Science at Tokyo Metropolitan University, Tokyo, Japan, in 1988, respectively. He was a researcher in the Department of Electrical Engineering at Tokyo Institute of Technology, Japan in 1985. Also, he was a visiting professor in the Department of Information Engineering at Nara Institute of Technology, Japan in 1997 and the Department of Information Engineering at University of Alberta, Canada in 2002 and a member of board of directors of NRF, Korea in 2012-2013. He is a professor in the Department of Computer Science and Statistics at Chosun University, Gwangju, Korea.

Choong-Ho Cho received B.S. and M.S. degrees from the Department of Industrial Engineering at Korea University, Seoul, Korea, in 1981 and 1983, respectively. He received M.S. and Ph.D. degrees from the Department of Computer Science at the Institute National des Sciences Appliques, Lyon, France, in 1986 and 1989, respectively. He was a postdoctoral fellow at INSA from 1989 to 1990. He was an assistant professor at Sooncheunhyang University from 1990 to 1994, and is currently a professor in the Department of Computer and Information Science at Korea University, Korea. His research interests include ubiquitous home networks, mobile/wireless networks, network traffic analysis, portable Internet, and wireless mesh networks.